# Factor Analysis of Dynamic Structures in Dynamic SPECT Imaging Using Maximum Entropy

A. Sitek, *Member, IEEE*, E.V.R. Di Bella, *Member, IEEE*,
and G.T. Gullberg, *Senior Member, IEEE*.
Medical Imaging Research Laboratory, University of Utah, Salt Lake City, Utah, USA

*Abstract*

Factor analysis of dynamic structures (FADS) is a technique used in the automatic extraction of time activity curves (TACs) from dynamic sequences. Although it has been reported that factor analysis with non-negativity constraints can in certain cases correlate with region of interest (ROI) measurements in SPECT and PET heart studies, the method does not ensure a unique solution. In this work it is shown that the FADS result is improved by using the Maximum Entropy Principle. Both the FADS technique and the new maximum entropy method were tested on simulated data and experimental $^{99m}$Tc-teboroxime canine cardiac data. The results showed that the FADS technique, using only non-negativity constraints, produced curves that did not always closely approximate the true curves. The new method, however, resulted in TACs that closely resembled the true curves. Thus, the inclusion of an entropy term is a useful method for obtaining more accurate extractions of TACs from dynamic SPECT data.

## I. INTRODUCTION

Factor analysis of dynamic structures [1-3] is a useful tool in the analysis of dynamic sequences. It can be used for automatic extraction of Time Activity Curves (TACs) from reconstructed dynamic heart images [4,5] as well as for extraction of TACs directly from dynamic projections with no prior reconstruction [6,7]. When performing a factor analysis on reconstructed images, typically principle component analysis is performed, then non-negativity constraints are imposed on the factors and the factor coefficients. The results of this procedure correlate with experimental region of interest (ROI) measurements of TACs in cardiac dynamic PET studies [4]. Unfortunately, a solution utilizing only non-negativity constraints is not mathematically unique. This has been a serious limitation of this technique.

In this work we employed the maximum entropy principle to improve the solutions obtained by FADS utilizing only non-negativity constraints. The idea of using the maximum entropy principle in factor analysis in medical imaging has been previously investigated [10]. In [10] a numerical study is presented in which the entropy of the factors and the entropy of the factor coefficients are maximized. The maximum entropy method in factor analysis has also been used in optics for estimation of component curves from unknown mixture spectra [8,9]. In this last approach however, the entropy was maximized only over the factors.

In the FADS method presented in this paper, a principal component analysis was performed first. Then, the entropy calculated over the factors was maximized concurrently with the imposition of non-negativity constraints on the principal component analysis factors and factor coefficients. The entropy was calculated only over the factors as in [8,9] because maximizing entropy over the factor coefficients, which lowers contrast in the factor coefficient images conflicts with maximizing entropy over the factors. It will be shown that contrast in factor coefficient images is increased in our study by including an entropy term. Results of computer simulations of the uptake of teboroxime-Tc-99m in the myocardium, and experimental results from a dynamic canine teboroxime-Tc-99m study are presented.

FADS was applied to a dynamic canine teboroxime-Tc-99m study because low count statistics in dynamic SPECT results in images that have very low spatial resolution, *i.e.*, there is a large overlap of regions with different temporal behavior, which makes it difficult to obtain correct TACs of these regions by ROI measurements. Also, the Compton scatter during the data acquisition affects ROI measurements. In order to minimize these effects the ROIs chosen must be small. However, even small ROIs do not completely eliminate the problem and small ROIs result in increased noise.

The goal of this work was to investigate the use of the maximum entropy principle for a better estimation of TACs, utilizing the FADS method.

## II. METHODS

### A. Factor Analysis of Dynamic Structures

The FADS method used in this paper consisted of two steps. The first step was a factor analysis of the data $A$, where the matrix $A$ of size $N \times M$ represented the dynamic sequence of images. $N$ was the number of

This work was supported by the NIH under Grant HL50663.

pixels in each image, and $M$ was the number of dynamic images. Each of these images correspond to a different time during the study. The data matrix $A$ was decomposed by performing the Singular Value Decomposition (SVD). Only the $K$ largest singular values were used and the others were set to zero. The number $K$ was chosen subjectively by examining the difference between each subsequent magnitude of singular values. The decomposed matrix $A$ could be expressed by:

$$A = C \cdot F. \tag{1}$$

The matrix $F$ was the matrix of factors of size $K \times M$, and $C$ was the matrix of the factor coefficients of size $N \times K$. The rows of $F$ were orthonormal and the columns of $C$ were orthogonal to each other.

Next the oblique rotation of the acquired matrices was performed in order to eliminate the negative values in both matrices. The rotation was done by estimating a rotation matrix $R$ of size $K \times K$ such that

$$A = CR^{-1} \cdot RF = \tilde{C} \cdot \tilde{F}. \tag{2}$$

As a result, matrices $\tilde{C} = CR^{-1}$ and $\tilde{F} = RF$, were non-negative. Given an $R$ that satisfied (2), the matrices $\tilde{C}$ and $\tilde{F}$ were determined within a scaling factor, *i.e.* any row of $\tilde{C}$ multiplied by any constant and corresponding column of $\tilde{F}$ multiplied by the reciprocal of this constant would give exactly the same $A$. To normalize the rotation matrix and eliminate this degree of freedom, the last column of the matrix $R$ had the following form:

$$\begin{aligned} R_{1K} &= 1 - (R_{11} + R_{12} + \ldots + R_{1K-1}) \\ &\cdots \\ R_{KK} &= 1 - (R_{K1} + R_{K2} + \ldots + R_{KK-1}) \end{aligned} \tag{3}$$

The matrix $R$ was found by minimizing the objective function which penalized the negativity of the matrices $\tilde{F}$ and $\tilde{C}$. As mentioned in the introduction, the result of the oblique rotation will not be unique when only the non-negativity constraint is used. To achieve better results with FADS, we used the maximum entropy principle by adding an entropy term to the objective function, $f(R)$:

$$f(R) = \alpha \cdot \sum_{\substack{i=1 \\ j=1}}^{N,K} H((CR^{-1})_{ij}) \cdot (CR^{-1})_{ij}^2 + \beta \cdot \sum_{\substack{i=1 \\ j=1}}^{K,M} H((RF)_{ij}) \cdot (RF)_{ij}^2 - \delta \cdot \sum_{\substack{i=1 \\ j=1}}^{K,M} -p_{ij} \cdot \log p_{ij} \tag{4}$$

where $\alpha$, $\beta$, and $\delta$ were positive scaling constants, and the function $H(x)$ was equal to 1 for $x < 0$ and 0 for $x \geq 0$. Also, $p_{ij}$ was defined as

$$p_{ij} = \frac{(RF)_{ij}}{\sum_{k=1}^{M} (RF)_{kj}} \tag{5}$$

The first two terms in Eq. (4) are the terms which penalize the negative elements of matrices $\tilde{C}$ and $\tilde{F}$. The third term in Eq. (4) is the entropy term. The entropy term has a minus sign since the entropy is maximized. The entropy term was calculated only over the factors and only the positive values of rotated factors, $(RF)_{kj}$ were taken into account during the calculation of the entropy term. The function $f(R)$ was minimized by using the Simplex Downhill method [12].

An important aspect of finding $R$ was the proper estimation of the coefficients $\alpha$, $\beta$, and $\delta$. Although there were three parameters, it was sufficient to estimate just the ratios between them since all three parameters contributed linearly to the objective function. The ratio $\alpha/\beta$ was determined by a short Monte Carlo simulation in which random matrices $R$ were generated. This simulation was done after the decomposition of the $A$ step, and before the minimization of $f(R)$, so it was specific to a given study. The ratio was chosen to be such that the average contribution to the objective function from the first and the second term of (4) calculated in the Monte Carlo simulation were the same ($\delta$ was equal to zero in this estimation). The value of the ratio $\delta/\beta$ was estimated based on the computer simulation of the MCAT phantom, and then the same ratio was used in the canine study.

TACs acquired by FADS were in normalized units, so in order to achieve quantitative results with true magnitudes, the curves had to be scaled by an appropriate scaling factor. Determination of this scaling factor is important in order to achieve quantitative results. The scaling factors in this paper were calculated

as the average value of the 3 highest coefficients of a given factor. Curves scaled in this way could be directly compared with ROI measurements which were also based on selecting the regions of the image with maximum amplitude. Wu *et al* [4] used a similar approach to extract scaling factors, but the scaling factor was calculated from the values above a certain threshold. Houston and Sampson [18] calculated scaling parameters in renal studies based on total count in the factor images, which required specifying the region over which the total count was calculated. We found, based on computer simulations, that our scaling approach gave quantitatively sound results.

*B. Computer Simulations*

Computer simulations were performed using the MCAT phantom [11]. A time series of images was created using a slice of the heart region of the MCAT phantom. Each image was 64x64 pixels and consisted of two factors: blood and myocardial tissue. The blood and myocardial tissue activity concentrations were formed to simulate the uptake of $^{99m}$Tc-teboroxime in the heart [13]. Background activity was assumed to be one-tenth of the blood pool activity; 183 dynamic images were simulated. Data was simulated with 50 realizations of 40% Gaussian noise (variance equal to 40% of the pixel value). To simulate the presence of vasculature arteries in the heart tissue 15% of the blood component was added to the simulated tissue curves [13]. Only a 20x19 pixel region encompassing the heart was analyzed.

The agreement between the curves found by minimizing (4) and the true activity curves was analyzed by calculating a norm of the curve difference. The curve difference was computed as the sum over all time points of the squared differences between the curves.

*C. Experimental Canine Studies*

Data from canine studies [15] were used to evaluate the factor analysis techniques. A three-detector scanner (PRISM 3000XP Picker International Inc., Cleveland, OH) with fan-beam collimators (65 cm focal length) was used to acquire transmission and emission projection data. The transmission scan was performed prior to the emission acquisition using a $^{153}$Gd fan-beam transmission line source. Without moving the canines, a bolus of $^{99m}$Tc-teboroxime was injected 5 seconds after the start of the dynamic acquisition. The camera acquired 120 projection angles every 5 seconds for 17 minutes. The 179 dynamic 3D images were reconstructed using 25 iterations of the ML-EM algorithm [16] with attenuation correction using attenuation maps that were determined by the transmission scan and scaled to the energy of $^{99m}$Tc. The reconstructed 3D images were then reoriented to obtain short-axis slices of the heart. Both factor analysis methods were applied to a 13x13 pixel region encompassing the myocardium in one short axis slice. The computation time for the optimization step was on the order of 15 seconds on a SPARC Station 3000. All of the factors were contained in this region. A small subregion was used because larger regions would contain additional components (*e.g.* liver). In analysis of these larger regions, the additional components could be neglected by zeroing the corresponding singular values, but it would lower the accuracy of the solution. Also, taking additional components into account would increase the complexity of the model.

The TACs extracted by the FADS methods were compared to curves obtained from manually chosen ROIs of four pixels. The blood input function was compared also to the measurement of the blood function by a blood flow probe. This probe consisted of an NaI detector placed on an arterial-venous shunt.

## III. RESULTS AND DISCUSSION

*A. Results of the computer simulations*

The effect of the entropy term in the objective function was investigated with computer simulations. Fig. 1 shows that with the entropy term, $\delta/\beta > 0$, the acquired blood curves agree better with the truth. That is, the norm between the curves and the truth was smaller. The norm rapidly decreased when $\delta/\beta > 0$, reached its minimum, and then slowly increased as $\delta/\beta$ increased. The entropy term had little effect on the tissue curves extracted by the FADS.

The comparison of the simulated curves with the TACs obtained by the FADS is presented in Figs. 2 and 3. The curves presented in Figs. 2 and 3 are results averaged over the 30 noise simulations. In Fig. 2 the large mismatch in the blood TACs between the result of the FADS with only non-negativity constraints and the true blood curve is shown. In Fig. 3, by using entropy, the blood curves match. In both of these cases (with and without entropy) the FADS tissue curves agreed with the simulated curves.

*B. Results of the experimental canine study*

At the beginning of the dynamic canine study, the bolus of the radioactivity first accumulates in the right ventricle, creating a sharp peak of increased activity in the right ventricle. This created an additional factor in the dynamic sequence which was taken into account. This factor will be referred to as the right ventricle (RV) factor. The results of the FADS method were compared to the ROI measurements and the blood

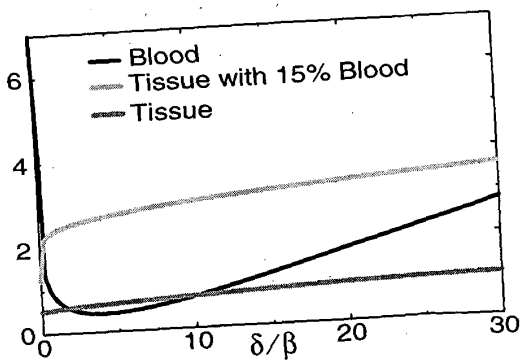


Figure 1. Value of the curve difference between the TACs obtained by FADS and the true curves *vs.* the different value of the ratio $\delta/\beta$. The darker gray line corresponds to the true tissue, and lighter gray line to the tissue with 15% of the blood component.

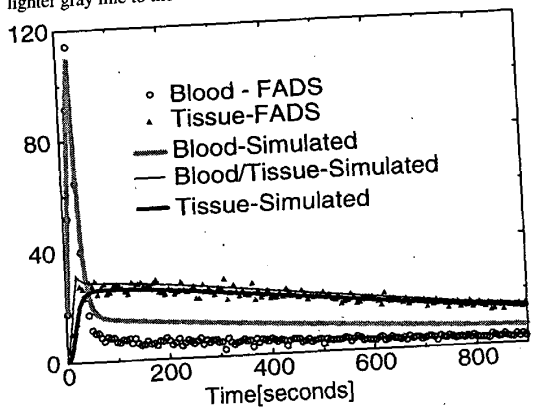


Figure 2. Comparison of the time activity curves acquired by FADS with only non-negativity constraints to the simulated curves.

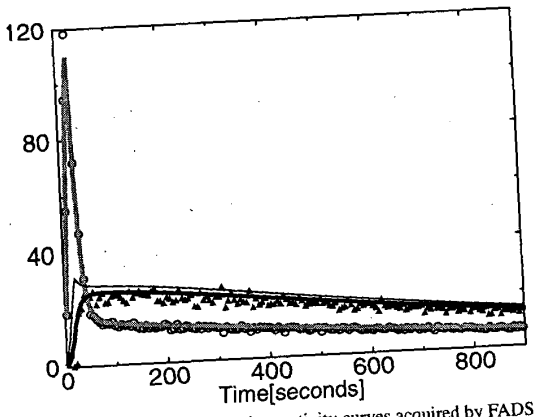


Figure 3. Comparison of the time activity curves acquired by FADS with non-negativity and entropy constraints to the simulated curves. Data for $\delta/\beta = 4$.

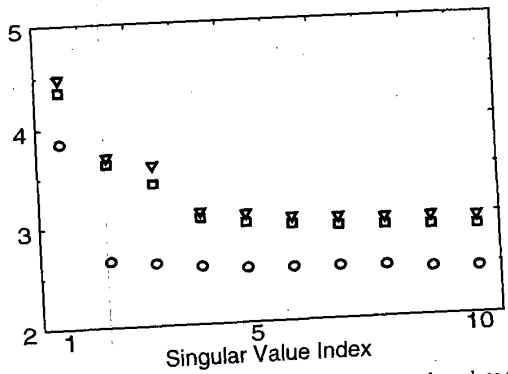


Figure 4. Values of the logarithm of the 10 largest singular values for 3 different canine studies. Circles correspond to the study presented in this paper. Triangles and squares correspond to other canine studies.

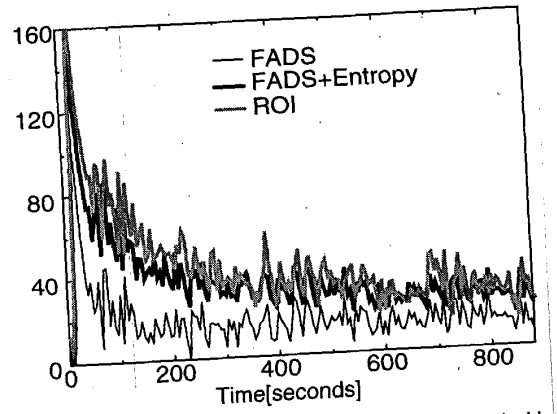


Figure 5. Comparison of the blood time activity curves acquired by FADS to curves obtained by the ROI measurements for the teboroxime-Tc-99m canine stress study.

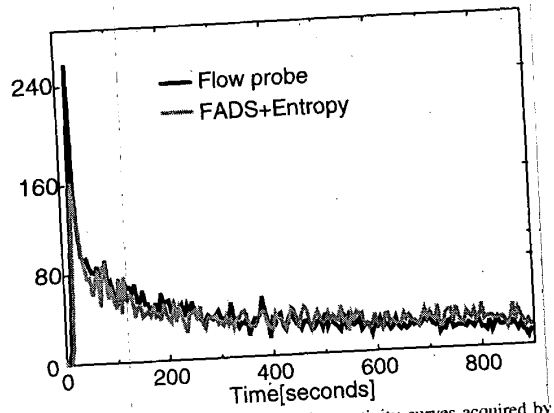


Figure 6. Comparison of the blood time activity curves acquired by FADS with entropy to the curves obtained by the blood flow probe measurements for the teboroxime-Tc-99m canine stress study (curves scaled to the same integral under the curves).

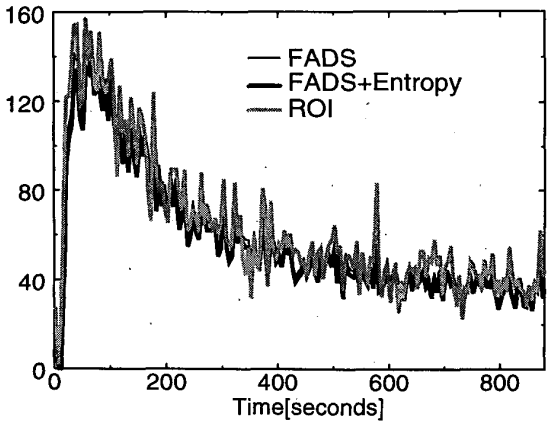


Figure 7. Comparison of the tissue time activity curves acquired by FADS to the curves obtained by the ROI measurements for the teboroxime-Tc-99m canine stress study.

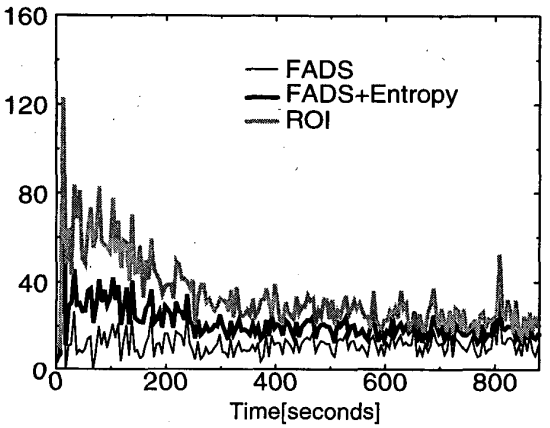


Figure 8. Comparison of the right ventricle time activity curves acquired by FADS to the curves obtained by the ROI measurements for the teboroxime-Tc-99m canine stress study.

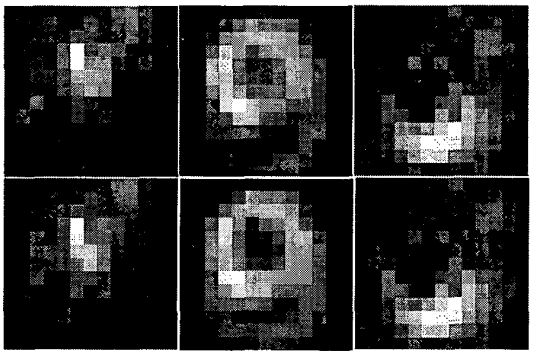

Figure 9. Images of factors extracted by FADS. The first column corresponds to the blood, the second to the tissue, and the third to the RV factor. The first row of images was obtained by FADS with non-negativity constraints, and the second row by FADS with entropy.

flow measurements. In Fig. 4 it can be seen that in some studies it was easy to determine using magnitudes of singular values, how many components were in the image, *e.g.*, 3 first components for studies corresponding to the triangles and the squares. It is clear that in these studies the first 3 singular values are much higher than the other values which are lower in magnitude. On the other hand it is not clear in the third case (circles). It is expected that in canine cardiac studies there will be 3 components. In this case it was not clear whether a fourth component should be used. However, by examining the structure of the factor curves and factor coefficients, we found that the coefficients for the third and fourth components were similar, but the fourth component did not bring additional structure and the corresponding singular value was small. Therefore, it was not used.

Figure 5 shows the comparison of the blood TACs extracted by the FADS to the ROI measurements. Similar to the simulations, the entropy term was needed to achieve agreement between the results of FADS and the ROI methods as shown in Fig. 5. The size of the ROI was only four pixels and as a result, FADS with entropy and ROI curves agree but the ROI curve is noisier. If larger ROIs are used, the curves will not match due to increased spillover in ROI curves. Figure 6 shows the comparison of the TACs obtained by the blood flow probe measurements with the TACs obtained by FADS with entropy. The figure shows the agreement between the TACs except at the beginning of the study where the curves differ in peak height. This difference is due to the poor temporal resolution of the dynamic SPECT acquisition.

In teboroxime-Tc-99m cardiac imaging, the availability of teboroxime in the blood for extraction is reduced by teboroxime binding [17]. The measured TACs of the blood- either by FADS, ROI, or flow probe- are thus not necessarily the blood input which should be used in estimation of kinetic parameters. However, it has been shown that wash-in $k_{21}$ 's estimated with blood input from ROIs correlate well with blood flow in canines [13].

Figures 7 and 8 present the comparison between tissue and RV curves obtained by FADS with the TACs obtained by ROI measurements. As in the computer simulations, the entropy only slightly affects the tissue curves obtained by FADS and they both agree with the ROI measurements. The ROI curves are noisier. Figure 8 shows that results of FADS and ROI measurements differ. This difference is due to increased spillover from tissue and blood in ROI measurements. This can be seen in Fig. 9 where the tissue and blood factor coefficient

images overlap with the RV. Also, in the same figure, the blood overlaps the tissue, but, as can be seen in Fig. 7, it does not affect the tissue curves. Figure 9 shows the images of the factor coefficients obtained by FADS. The contrast in the image of the tissue factor was increased by use of an entropy term calculated over the factors. That means that by maximizing entropy calculated over factors, the entropy of factor coefficients is lowered.

## IV. CONCLUSIONS

A maximum entropy term was used with the FADS method for the extraction of TACs from a time series of images acquired by dynamic SPECT. We showed that the agreement between the true curves and the TACs obtained by the FADS method in computer simulations was improved by the utilization of a maximum entropy term in the objective function. Also, curves obtained by ROIs and flow probe blood measurements showed better correlation with the TACs obtained by the FADS when the entropy term was used. It has been shown [5] that the effects of non-uniqueness in the FADS method are especially prevalent in the blood component and are not as prevalent in the tissue curves. The work in this paper confirms these findings and it shows that utilization of an entropy term removes the ambiguity of the FADS when extracting the blood input function. The method improves the accuracy of the FADS acquired blood curves yet does not affect the tissue curves that do not suffer from non-uniqueness effects. Additionally, the use of the entropy term improved the contrast in the tissue factor coefficient images.

## V. ACKNOWLEDGEMENTS

The authors would like to thank Sean Webb for editing the manuscript.

## V. REFERENCES

[1] D. C. Barber, "The use of principal components in the quantitative analysis of gamma camera dynamic studies," *Phys. Med. Biol.* **25**, pp. 283-292, 1980.

[2] M. Samal, M. Karny, H. Surova, E. Marikova, and Z. Dienstbier, "Rotation to simple structure in factor analysis of dynamic radionuclide studies," *Phys. Med. Biol.* **32**, pp. 371-382, 1987.

[3] I. Buvat, H. Benali, F. Frouin, J. P. Bazin, and R. Di Paola,"Target apex-seeking in factor analysis of medical image sequences," *Phys. Med. Biol.* **38**, pp. 123-138, 1993.

[4] H-M. Wu, C. K. Hoh, Y. Choi, H. R. Schelbert, R. A. Hawkins, M. E. Phelps, and S. C. Huang, "Factor analysis for extraction of blood time-activity curves in dynamic FDG-PET studies," *J. Nucl. Med.*, vol. **36**, pp. 1714-1722, 1995.

[5] A. Sitek, E. V. R. DiBella, and G. T. Gullberg, "Factor analysis of dynamic structures in cardiac dynamic SPECT," submitted to *Phys. Med. Biol.*, 1999.

[6] A. Sitek, E. V. R. DiBella, and G. T. Gullberg, "Direct extraction of tomographic time activity curves from dynamic SPECT projections using factor analysis," *J. Nucl. Med.*,vol. **39**, p. 144P, 1998.

[7] A. Sitek, E. V. R. DiBella, and G. T. Gullberg, "Reconstruction from slow rotation dynamic SPECT using a factor model," in 1999 IPMI Conference Record, *Lecture Notes in Computer Science*, vol. **1613**, pp. 436-441, Springer (Eds. A. Kuba *et al*) 1999.

[8] K. Sasaki, S. Kawata, and S. Minami, "Estimation of component spectral curves from unknown mixture spectra," *Appl. Opt.*, vol. **23**, pp. 1955-1959, 1984.

[9] K. Sasaki, S. Kawata, and S. Minami, "Constrained nonlinear method for estimating component spectra from multicomponent mixtures," *Appl. Opt.*, vol. **22**, pp. 3599-3603, 1983.

[10] M. Nakamura, Y. Suzuki, and S. Kobayashi, "A method for recovering physiological components from dynamic radionuclide images using the maximum entropy principle: A numerical investigation," *IEEE Trans. Biomed. Eng.*, vol. **36**, pp. 906-916, 1989.

[11] B. M. W. Tsui, J. A. Terry, and G. T. Gullberg, "Evaluation of cardiac cone-beam SPECT using observer performance experiments and ROC analysis," *Investigative Radiology*, vol. **28**, pp. 1101-1112, 1993.

[12] J. A. Nelder and R. Mead, "A simplex method for function minimization," *Comp. J.*, vol. **7**, pp. 308-313, 1964.

[13] A. Smith, G. T. Gullberg, and B. S. Christian, "Experimental verification of technetium 99m-labeled teboroxime kinetic parameters in the myocardium with dynamic single-photon emission computed tomography: Reproducibility, correlation to flow, and susceptibility to extravascular contamination," *J. Nucl. Cardiol.*, vol. 3, pp. 130-142, 1996.

[14] W. H. Press, S. A. Teukolsky, W. T. Vetterling, and B. P. Flannery, "*Numerical Recipes in C*," Cambridge University Press, pp. 420-425, 1993.

[15] E. V. R. Di Bella, S. G. Ross, G. T. Gullberg, and P.E. Christian, "Myocardial blood flow measurements using compartmental modeling of technetium 99m-labeled teboroxime: Comparision to static Tl-201," submitted to *Eur. J. Nucl. Med.*, 1999.

[16] L.A. Shepp and Y. Vardi, "Maximum likelihood reconstruction for emission tomography," *IEEE Trans Med. Imag.*, vol. MI-**1**, pp. 113-122, 1981.

[17] W.L. Rumsey, K. C. Rosenspire, and A. D. Nunn, "Myocardial extraction of teboroxime: Effects of teboroxime interaction with blood," *J. Nucl. Med.*, vol. **33**, pp. 94-101, 1992.

[18] A.S. Houston and W.F.D. Sampson, "A quantitative comparison of some FADS methods in renal dynamic studies using simulated and phantom data," *Phys. Med. Biol.*, vol. **42**, pp. 199-217, 1997.